

This is the accepted manuscript made available via CHORUS. The article has been published as:

## Circular dichroism in high-order harmonic generation from chiral molecules

Yoichi Harada, Eisuke Haraguchi, Keisuke Kaneshima, and Taro Sekikawa

Phys. Rev. A **98**, 021401 — Published 3 August 2018

DOI: [10.1103/PhysRevA.98.021401](https://doi.org/10.1103/PhysRevA.98.021401)

# Circular dichroism in high harmonic generation from chiral molecules

Yoichi Harada, Eisuke Haraguchi, Keisuke Kaneshima, and Taro Sekikawa\*

*Department of Applied Physics, Hokkaido University, Kita 13 Nishi 8, Kita-ku, Sapporo 060-8628, Japan*

*\*Corresponding author: [sekikawa@eng.hokudai.ac.jp](mailto:sekikawa@eng.hokudai.ac.jp)*

## Abstract

In this study, circularly polarized high harmonic generation (CP-HHG) from a chiral molecule, limonene, by a CP counter-rotating two-color laser field was found to possess circular dichroism. A high harmonic spectrum from a limonene enantiomer depends on the combination of the chirality of the enantiomer and the rotation direction of the superimposed two-color laser field in comparison with that of an achiral atom, helium. From *R*-enantiomer, the harmonic orders with clockwise polarization were generated more efficiently than those with counterclockwise polarization and vice versa. CP-HHG can be a sensitive probe of the chirality of biomolecules on the femtosecond and attosecond timescales.

Chiral molecules are not superimposable on their mirror images, called enantiomers. They do not have a symmetry plane nor a center of inversion symmetry. Although the physical properties of the enantiomers are the same, the chemical reactivity of chiral molecules exhibits a strong enantiomeric selectivity. Therefore, the chirality plays a decisive role in biological systems. Discerning the enantiomers is important for understanding the activities of chiral molecules in biological systems.

To distinguish between the enantiomers in a condensed phase, optical approaches such as the circular dichroism (CD) of photoabsorption and the optical rotation of light polarization have been used. These effects are induced by the interference term  $\vec{\mu} \cdot \vec{m}$  between the electric  $\vec{\mu}$  and magnetic  $\vec{m}$  dipoles in the transition moment [1]. As  $|\vec{m}|$  is generally small, the magnitude of the CD of photoabsorption is typically on the order of  $10^{-4}$ – $10^{-5}$ . Therefore, discerning the enantiomers is a demanding task. However, in the gas phase, the spatial distribution of the photoelectron emission from chiral molecules was found to have a larger anisotropy than the CD of photoabsorption by two or three orders of magnitude, enabling the observation or determination of the molecular chirality with a higher sensitivity [2-5].

Recently, using another approach based on high harmonic generation (HHG), the observation of molecular chirality was reported [6]. HHG is based on nonlinear interactions between a laser electric field and the interacting molecules [7]. The process of HHG is intuitively understood by the three-step model, where an electron 1) is ionized by tunneling from an atom or molecule in the presence of a strong laser field, 2) is accelerated in the laser field, and 3) recombines with the parent ion and then emits a higher harmonic photon with an energy corresponding to the sum of the kinetic and ionization energies [8]. Because the HHG yield depends on the electronic states of the interacting molecules through tunneling and recombination probabilities, HHG can be used to probe the electronic states of the molecules, including the symmetry or the chirality of the molecular orbitals. This spectroscopic approach is known as high harmonic spectroscopy (HHS).

In Ref. [6], HHS was applied to detect the chirality based on the observation that the HHG yield from chiral molecules is asymmetric with respect to the sign of the degree of the ellipticity of the driving laser.

The ellipticity maximizing the anisotropy was found to be  $\pm 1\text{--}2\%$ . This anisotropy comes from the transition between electronic states in the cation, dependent on  $\bar{m}$  pertinent to the molecule, during the second step of the three-step model. The recombining state of the cation with the free electron during the third step could be different from the initial state upon tunneling ionization, resulting in a difference in HHG yield. The interstate transition during the second step is sensitive to the sign of  $\bar{m}$ . Thus, the HHG yield is chiral-sensitive.

In this work, we investigated the CD of the circularly polarized HHG (CP-HHG) by a two-color bicircular laser field [9-18] from chiral molecules. CP-HHG from a single-color single CP laser beam is prohibited by the conservation of spin angular momentum. Considering the three-step model, the released electron cannot return to the parent ion under a CP light field, resulting in no HHG. Therefore, in Ref. [6], the polarization of the laser pulses used was very close to linear, as described above. In contrast, a two-color CP laser field with counter-rotating polarizations generates CP high harmonic pulses. The synthesized laser field by the fundamental ( $\omega$ ) and its second-harmonic ( $2\omega$ ) CP light exhibits a threefold spatiotemporal symmetry. Therefore, the  $3m$ -order harmonics are missing in isotropic media, where  $m$  is a positive integer [11,13]. The circular polarizations of the  $3m+1$  and  $3m+2$  harmonics are the same as those of  $\omega$  and  $2\omega$ , respectively, and are opposite to each other because of the conservation of spin angular momentum.

In the quantum mechanical expression of the three-step model of HHG, the third step is expressed as the complex conjugate of the transition dipole moment between the ground state and ionized state [9,12,15,19,20]. Therefore, the CP-HHG yield is expected to depend on the symmetry of the wavefunction of the outermost atomic or molecular orbital [9,12]. Experimentally, the relative intensities of the allowed neighboring harmonics,  $3m+1$  and  $3m+2$ , were found to depend on the atomic species [15,17]. In the early stage of the investigation, these relative intensities appeared to be understood by the following propensity rule: Single photoionization with a field corotating with the initial state is much more likely than with a counter-rotating field [12,15]. However, the underlying

mechanism was found to be more complicated, and precise theoretical calculations are necessary to understand it completely [17].

Although the quantitative prediction of the relative intensities is not simple, the sensitivity of CP-HHG to the outermost atomic orbital suggests that CP-HHG is also susceptible to the highest occupied molecular orbital (HOMO) of a chiral molecule, the direction of which should be determined by the rotation direction of the electrons in the HOMO. Even for randomly oriented molecules, the chirality is active. This indicates that CP-HHG can be used to discern molecular chirality. Still, the response of a large molecule to a laser field would not be as simple as that of an atomic orbital. Therefore, the purpose of the present work is the experimental exploration of the sensitivity of CP-HHG to molecular chirality.

For this purpose, the CP-HHG spectra from the enantiomers of 1-methyl-4-(prop-1-en-2-yl)cyclohex-1-ene (limonene, inset of Fig. 1) were observed. These enantiomers act differently in our bodies, e.g., each enantiomer has a peculiar smell: *R*- and *S*-limonene have the fragrance of oranges and pine, respectively. When light with a linear polarization passes through a pure enantiomer, the plane of polarization is rotated [21]. This is known as optical rotation. *R*- or *S*-limonene molecules rotate the plane clockwise or counterclockwise as viewed by an observer facing the oncoming wave, respectively.

The experimental setup for CP-HHG is illustrated in Fig. 1. A Ti:sapphire laser system delivers 1.4-mJ, 35-fs pulses with a center wavelength of 800 nm at a repetition rate of 1 kHz. The two-color counter-rotating CP laser field was synthesized by the inline setup called MAZEL-TOV [22]: The linearly polarized 800-nm pulses were partially converted to 400-nm pulses with a polarization perpendicular to  $\omega$  by a  $\beta$ -BaB<sub>2</sub>O<sub>4</sub> (BBO) crystal with a thickness of 300  $\mu$ m. The pulse energies of the  $\omega$  and  $2\omega$  pulses were 0.9 and 0.5 mJ, respectively. After compensating the group-delay between the  $\omega$  and  $2\omega$  pulses by two calcite plates, their polarizations were changed to circular by a superachromatic quarter-waveplate (SAQW) (RSU1.4.15, Bernhard Halle Nachf. GmbH). Here, the rotation directions of the  $\omega$  and  $2\omega$  were opposite to each other and were switched just by rotating the crystal axis of the SAQW by 90°. Because of the inline setup, the spatial overlap between the  $\omega$  and  $2\omega$  beams was suitable to form

a triangular electric field. The generation of the  $3m$ -order harmonics was almost suppressed. In this paper, counterclockwise polarization is defined by an observer facing an oncoming wave and vice versa.

The two-color synthesized laser field was focused into a gas jet using a concave mirror with a focal length of 0.5 m. The gas jet was formed by a glass capillary with an inner diameter of 300  $\mu\text{m}$ . The capillary tip was set at the focal point of the mirror. The peak intensities of the  $\omega$  and  $2\omega$  beams were estimated to be  $5.0 \times 10^{14}$  and  $1.4 \times 10^{14}$  W/cm<sup>2</sup>, respectively. The enantiomers of limonene molecules, purchased from Wako Pure Chemical Industries Ltd., were stored in a glass bubbler and warmed to 358 K to increase their vapor pressure. The limonene vapor was sent through a heated pipeline to the glass capillary mixed with 1.6-atm helium gas. The flow of the limonene molecules mixed with helium was continuous.

The spectra of the high harmonics were recorded by a magnetic bottle photoelectron spectrometer after converting the high harmonic photons into photoelectrons from krypton gas. The intensity of each harmonic was obtained by integrating the counts of each peak, and the ambiguity of the intensity was estimated by the square root of the total counts. The photoelectron spectrometer was used because of the availability of the experimental apparatus. Note that the photoelectron spectra of krypton possess two peaks for each harmonic order because of the spin-orbit splitting to the  $^2P_{3/2}$  and  $^2P_{1/2}$  states of the cation. The intensity ratio is expected to be approximately 2:1 from the degeneracy of the states. However, the collection efficiency and energy resolution of the photoelectron spectrometer depend on the kinetic energy [23]. Therefore, the observed spectra of the photoelectron peaks were not necessarily as expected.

Figures 2a, 2b, and 2c present the spectra of the CP-HHG from helium, *S*-limonene, and *R*-limonene, respectively. The red clockwise (blue counterclockwise) circular arrow in Fig. 2 indicates the rotation direction of the polarization of the  $\omega$  ( $2\omega$ ) used for HHG. The green dotted (yellow solid) lines indicate the CP-HHG spectra generated by the combination of a clockwise (counterclockwise) rotating  $\omega$  and counterclockwise (clockwise) rotating  $2\omega$  represented by the red and blue arrows, respectively. The following three features in the spectra are identified: 1) The spectral changes of the helium signal with

the rotational direction of the polarization are small in comparison to the limonene signal. 2) The  $3m+1$  harmonics of the *R*-limonene signal are relatively more enhanced than the  $3m+2$  when the  $\omega$  has a clockwise polarization. 3) However, for the counterclockwise polarization of the  $\omega$ , the  $3m+1$  harmonics of the *S*-limonene signal are more enhanced.

To quantitatively evaluate the CD, the Kuhn g-factor  $2(I_L - I_R)/(I_L + I_R)$ , where  $I_L$  and  $I_R$  are the intensities with counterclockwise and clockwise polarization, respectively, was estimated by summing up the counts for each harmonic order after normalizing the total counts of the observed spectrum to the same value for each polarization and is shown in Fig. 3a. *R*-limonene (triangle) generates more high harmonics with clockwise circular polarization than with counterclockwise circular polarization, while *S*-limonene (circle) prefers the generation of harmonics with counterclockwise circular polarization. The Kuhn g-factors are almost symmetrical with respect to the baseline, indicating the CD in HHG.

However, there is concern regarding the degree of circular polarization of the driving laser created by the SAQW, because the SAQW inevitably has a certain amount of deviation from an ideal waveplate both in retardation and in the crystal axis. In fact, the HHG spectra from helium change slightly with polarization, as shown in Fig. 2a. In addition, the 18th harmonic is still observed, although the optimal angles of the SAQW were adjusted using argon gas, yielding more intense high harmonics. This suggests that the symmetry of the superimposed electric field deviated from the threefold symmetry and that the rotation of the SAQW did not necessarily switch the rotational direction of the polarization mirror symmetrically. In addition, the displacement between the  $\omega$  and  $2\omega$  beams caused by the refraction inside the SAQW consisting of several birefringent plates may also have differed when the SAQW was rotated.

To examine the CD in CP-HHG using an independent approach, the spectra of the limonene signal were compared to those of helium, since the CP-HHG spectra from helium do not depend on the rotating direction of the polarization, because of the *s* symmetry of its outermost atomic orbital. The spectral changes induced by exchanging the gas media under the same polarization should be attributable to the helicity of the HOMO wavefunction of the enantiomer.

The integrated intensity ratio between the *R*-(*S*-) limonene and helium signal for each harmonic order is shown in Fig. 3b (3c). Here, the total observed signals from limonene and from helium have been normalized to the same value so that the intensity ratios are distributed at about unity. If the CP-HHG spectra are identical to those from helium, these ratios should be constant with respect to the harmonic orders. However, in *R*-(*S*-) limonene, for example, the ratios at  $3m+1$  are larger than those at  $3m+2$  using the clockwise (counterclockwise)  $\omega$  laser field. These relationships are reversed from an enantiomer using the opposite circular polarization. These results demonstrate the CD in HHG from chiral molecules.

However, the changes of the intensity ratios of the 20th harmonic from those of the 19th harmonic are not clear because of experimental ambiguity in Figs. 3b and 3c, although the Kuhn *g*-factor exhibits dichroism. Further data accumulation will clarify the difference from the helium signal. Another possible reason is the incomplete polarization switching by the SAQW, as described above. Hence, the Kuhn *g*-factor may have a systematic error and the ambiguities of Kuhn *g*-factors might be larger than the estimated error bars, which will also be clarified by improving the signal-to-noise ratio.

Under the present experimental conditions, the interaction length between the laser field and chiral molecules was 300  $\mu\text{m}$  and the gas density of the chiral molecules was low. Therefore, the phase-mismatch among the driving laser pulses and high harmonic pulses was negligible [13,15,24], which will be evaluated later. The response of a single molecule should be crucial for dichroism. The observed CD would be explained by the same processes proposed in Refs. [6] and [20]: The transition to another state by  $\bar{m}$  in the cation during the second step of the three-step model modulates the efficiency of HHG.

Here, however, more intuitive perspectives may be provided. One is the propensity rule of the ionization probability dictating the third process of the three-step model [12,15,17]: The emitted radiation is more likely to acquire a polarization with the same rotation direction of the outermost atomic orbitals [12]. Therefore, the preferred CP-HHG is determined by the rotation direction of the HOMO wavefunction of an enantiomer.



As another perspective, the resonance with the intermediate states with CD could be responsible for the CD in HHG. In perturbative nonlinear optics, it is well-known that the resonance with the electronic states of nonlinear media enhances the nonlinear susceptibility. Even in HHG, the resonance with an electronic state raises the generation efficiency [25]. The photoabsorption of limonene appears in a wavelength region shorter than about 220 nm with CD [26]. Thus, both  $\omega$  and  $2\omega$  can be resonant with the states at 200 nm. Because *R*-limonene has a larger absorption coefficient for clockwise polarization at 200 nm [26], the nonlinear responses to the clockwise polarized light could be larger at 200 nm than to the counterclockwise polarization. Experimentally, the Kuhn *g*-factors are found to have a negative sign for *R*-limonene, as shown in Fig. 3a. That is, the high harmonics with clockwise polarization were generated more efficiently from *R*-limonene. Considering that the  $3m+1$  and  $3m+2$  orders have the same polarization as  $\omega$  and  $2\omega$ , respectively [13], the resonance of  $\omega$  or  $2\omega$ , with clockwise polarization, with the dichroic states enhances the high harmonics with clockwise polarization from *R*-limonene.

CD of the states at about 200 nm in limonene was observed in the photoelectron spatial distribution: Fanood et al. observed the wavelength dependence of the anisotropy of the photoelectron emission by the (2+1) resonance multiphoton ionization by the CP photons [27]. They found that the sign of the asymmetry factor of the photoemission from the HOMO was reversed when the center wavelength of the laser was changed from 420 to 392 nm. Interestingly, at these wavelengths, the sign of the CD of linear absorption also reversed [26]. This correspondence between the CD of the photoelectron emission and that of the linear absorption is attributed to the resonance with different vibrational levels and different electronic ion core configurations in the intermediate Rydberg states [27]. The intermediate states with CD should also influence the HHG through the resonance effects.

The enhancement of CP-HHG by the resonance with the intermediate states with CD also appears to be the case in Ref. [6]. It was found that an elliptically polarized driving laser rotating in the clockwise direction with photon energies of 0.70 and 0.67 eV generates high harmonics more efficiently from *S*-epoxypropane and *R*-fenchone than the laser field rotating in the opposite direction. According to Refs. [28] and [29], *S*-epoxypropane and *R*-fenchone are resonant and have larger absorption coefficients at

11 (= 7.7 eV) and 6 photons (= 4.0 eV) for the clockwise polarization, respectively. The correspondence found in limonene predicts that high harmonics are generated more efficiently by the driving laser with the clockwise polarization from these enantiomers, and successfully explains the experimental observation.

Finally, the phase mismatch in CP-HHG was estimated as follows. The angle of the optical rotation  $\alpha$  and the difference in the refractive indices of the circular polarizations  $\Delta n$  have the relation of  $\alpha = \pi \Delta n l / \lambda$ , where  $\lambda$  and  $l$  are the wavelength and interaction length, respectively. Using  $\alpha$  and  $n$  given in Ref. [21],  $\Delta n$  at  $\omega$  and  $2\omega$  was deduced to be  $2.1 \times 10^{-6}$  and  $5.2 \times 10^{-6}$ , respectively, for a 1-cm-long liquid. As  $\Delta n$  is proportional to the density of limonene,  $\Delta n$  in the gas phase was estimated considering the vapor pressure [30]; at 358 K, the vapor pressure was 4.92 kPa. If the total gas pressure just below the capillary tube was 2700 Pa [31], the pressure of limonene would be estimated as 82 Pa. When the temperature was cooled to 100 K by supersonic expansion, the gas density of limonene was  $1.4 \times 10^{-5}$  g/cm<sup>3</sup>. As  $\Delta n$  is proportional to the density and the interaction length  $L$  of 300  $\mu$ m,  $\Delta n$  at  $2\omega$  and  $\omega$  are  $8.2 \times 10^{-11}$  and  $3.3 \times 10^{-11}$ , respectively. Meanwhile, the corresponding average refractive indices are 1.00026 and 1.00025, respectively. Therefore, under the assumption that the refractive indices in the extreme ultraviolet range are unity, the difference in the phase mismatch coming from the CD is negligibly small and phase matching is not the primary effect.

In summary, the CP-HHG limonene enantiomer spectra were found to exhibit CD in the intensities relative to those from helium atoms. CP-HHG is sensitive to the chirality of the interacting molecules with a synthesized CP light field. CP-HHG appears to be very promising for discriminating enantiomers. As CP-HHG includes processes taking place on the attosecond timescale, CP-HHG might also be applicable to probe the attosecond transient chirality of molecules.

We acknowledge funding from JST CREST (Grant Number JPMJCR15N1) and KAKENHI (Grant Numbers 15H03702 and 16K13854), Japan.

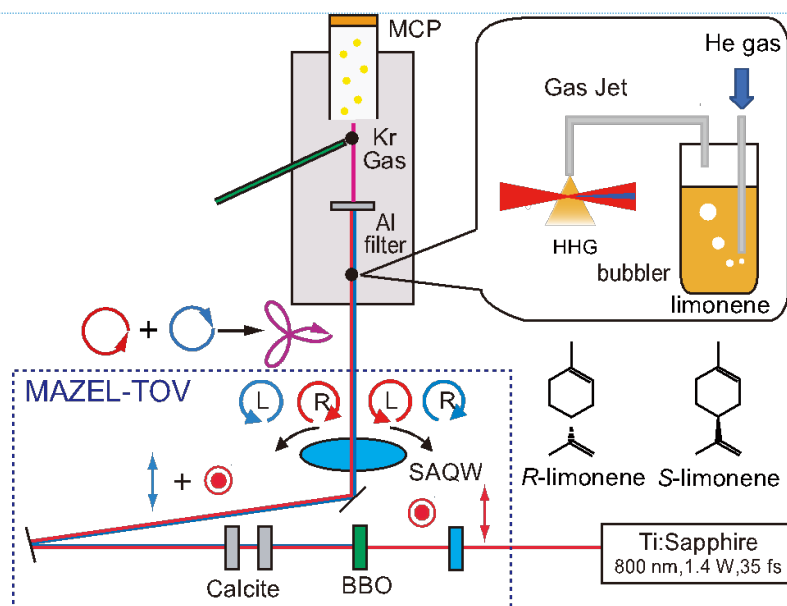


Fig. 1. Experimental setup for the observation of CP-HHG. MAZEL-TOV is the optical system used to generate the two-color counter-rotating CP laser field consisting of a BBO crystal, calcite plates, and a SAQW [22]. The superposition of the two-color counter-rotating polarized laser fields, of which the rotation directions of the fundamental and second-harmonic light field are represented by the counterclockwise (red) and clockwise (blue) arrows, respectively, forms triangular polarization with threefold symmetry, represented by the purple arrow.

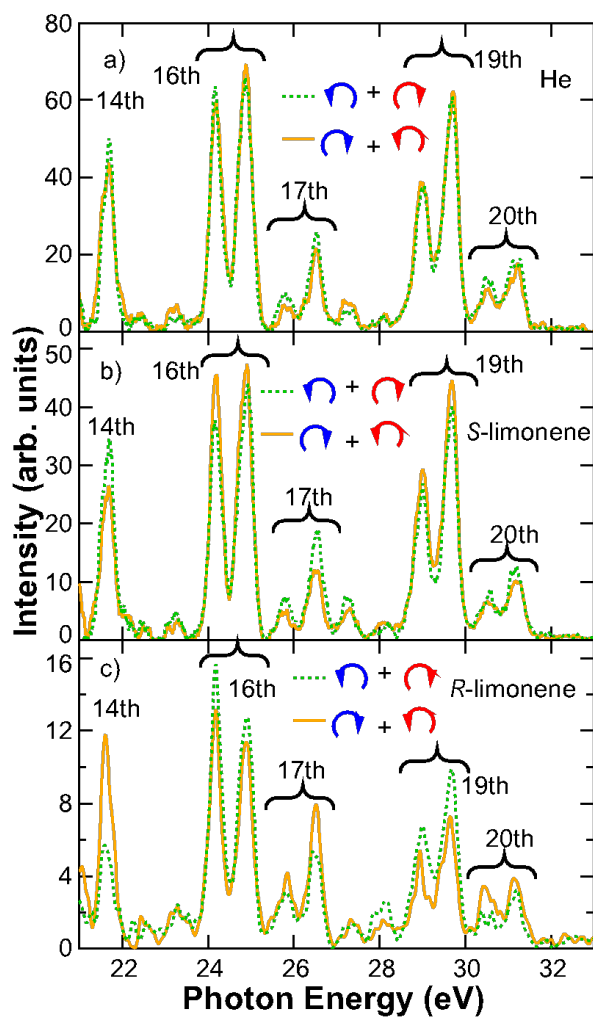


Fig. 2. High harmonics spectra from (a) He, (b) *S*-limonene, and (c) *R*-limonene, generated by the synthesized laser field by the CP  $\omega$  and  $2\omega$ . The spectra shown by the green dotted (orange solid) lines have been generated by the combination of  $\omega$  and  $2\omega$ , of which the rotational directions of the polarization are clockwise (counterclockwise), represented by red arrow, and counterclockwise (clockwise), represented by blue arrow, respectively.

Deleted: 1

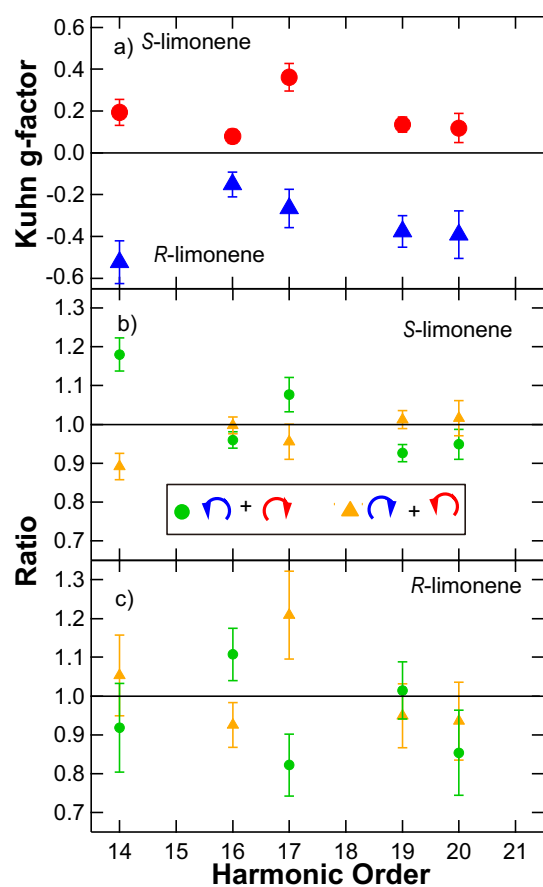


Fig. 3. (a) Kuhn g-factors from the enantiomers for each higher harmonic order. (b, c) Intensity ratio of each high harmonic from limonene enantiomers and helium. The solid circles and triangles have been obtained by the clockwise and counterclockwise  $\omega$  in combination with the counter-rotating  $2\omega$ , respectively.

## Reference

- [1] P. Fischer and F. Hache, *Chirality* **17**, 421 (2005).
- [2] B. Ritchie, *Phys. Rev. A* **13**, 1411 (1976).
- [3] N. Böwering, T. Lischke, B. Schmidtke, N. Müller, T. Khalil, and U. Heinzmann, *Phys. Rev. Lett.* **86**, 1187 (2001).
- [4] T. Lischke, N. Böwering, B. Schmidtke, N. Müller, T. Khalil, and U. Heinzmann, *Phys. Rev. A* **70**, 022507 (2004).
- [5] M. H. M. Janssen and I. Powis, *Phys. Chem. Chem. Phys.*, **16** (2014).
- [6] R. Cireasa, A. E. Boguslavskiy, B. Pons, M. C. H. Wong, D. Descamps, S. Petit, H. Ruf, N. Thiré, A. Ferré, J. Suarez *et al.*, *Nature Phys.* **11**, 654 (2015).
- [7] F. Krausz and M. Ivanov, *Rev. Mod. Phys.* **81**, 163 (2009).
- [8] P. B. Corkum, *Phys. Rev. Lett.* **71**, 1994 (1993).
- [9] D. B. Milošević, W. Becker, and R. Kopold, *Phys. Rev. A* **61**, 063403 (2000).
- [10] A. Fleischer, P. Sidorenko, and O. Cohen, *Opt. Lett.* **38**, 223 (2013).
- [11] A. Fleischer, O. Kfir, T. Diskin, P. Sidorenko, and O. Cohen, *Nature Photon.* **8**, 543 (2014).
- [12] L. Medišauskas, J. Wragg, H. van der Hart, and M. Y. Ivanov, *Phys. Rev. Lett.* **115**, 153001 (2015).
- [13] O. Kfir, P. Grychtol, E. Turgut, R. Knut, D. Zusin, D. Popmintchev, T. Popmintchev, H. Nembach, J. M. Shaw, A. Fleischer *et al.*, *Nature Photon.* **9**, 99 (2015).
- [14] T. Fan, P. Grychtol, R. Knut, C. Hernández-García, D. D. Hickstein, D. Zusin, C. Gentry, F. J. Dollar, C. A. Mancuso, C. W. Hogle *et al.*, *Proc. Natl. Acad. Sci. USA* **112**, 14206 (2015).
- [15] D. Baykusheva, M. S. Ahsan, N. Lin, and H. J. Wörner, *Phys. Rev. Lett.* **116**, 123001 (2016).
- [16] D. Wang, X. Zhu, L. L. Xi Liu, X. Zhang, P. Lan, and P. Lu, *Opt. Express* **25**, 23502 (2017).
- [17] D. Baykusheva, S. Brennecke, M. Lein, and H. J. Wörner, *Phys. Rev. Lett.* **119**, 203201 (2017).
- [18] Á. Jiménez-Galán, N. Zhavoronkov, M. Schloz, F. Morales, and M. Ivanov, *Opt. Express* **25**, 22880 (2017).
- [19] M. Lewenstein, P. Balcou, M. Y. Ivanov, A. L'Huillier, and P. B. Corkum, *Phys. Rev. A* **49**, 2117 (1994).
- [20] O. Smirnova, Y. Mairesse, and S. Patchkovskii, *J. Phys. B: At. Mol. Opt. Phys.* **48**, 234005 (2015).
- [21] E. O. Hulburt, *Astrophys. J.* **54**, 116 (1921).
- [22] O. Kfir, E. Bordo, G. I. Haham, O. Lahav, A. Fleischer, and O. Cohen, *Appl. Phys. Lett.* **108**, 211106 (2016).
- [23] P. Kruit and F. H. Read, *J. Phys. E: Sci. Instrum.* **16**, 313 (1983).
- [24] O. Kfir, P. Grychtol, E. Turgut, R. Knut, D. Zusin, A. Fleischer, E. Bordo, T. Fan, D. Popmintchev, and T. Popmintchev, *J. Phys. B: At. Mol. Opt. Phys.* **49**, 123501 (2016).
- [25] E. S. Toma, P. Antoine, A. d. Bohan, and H. G. Muller, *J. Phys. B: At. Mol. Opt. Phys.* **32**, 5843 (1999).
- [26] P. Brint, E. Meshulam, and A. Gedanken, *Chem. Phys. Lett.* **109**, 383 (1984).
- [27] M. M. R. Fanoood, M. H. M. Janssen, and I. Powis, *J. Chem. Phys.* **145**, 124320 (2016).
- [28] M. Carnell, S. D. Peyerimhoff, A. Breest, K. H. Gödderz, P. Ochmann, and J. Hormes, *Chem. Phys. Lett.* **180**, 477 (1991).
- [29] F. Pulm, J. Schramm, J. Hormes, S. Grimme, and S. D. Peyerimhoff, *Chem. Phys.* **224**, 143 (1997).
- [30] M. F. Rodrigues and M. G. Bernardo-Gil, *J. Chem. Eng. Data* **40**, 1193 (1995).
- [31] T. Adachi, K. Kondo, and S. Watanabe, *Appl. Phys. B* **55**, 323 (1992).

Deleted: 1